Ab Initio and Improved Empirical Potentials for the Calculation of the Anharmonic Vibrational States and Intramolecular Mode Coupling of *N*-Methylacetamide

Susan K. Gregurick*

Department of Chemistry and Biochemistry, University of Maryland, Baltimore County, 1000 Hilltop Circle, Baltimore, Maryland 20215

Galina M. Chaban

NASA Ames Research Center, Mail Stop T27B-1, Moffett Field, California 94035-1000

R. Benny Gerber

Department of Physical Chemistry and the Fritz Haber Research Center, The Hebrew University, Jerusalem 91904, Israel, and Department of Chemistry, University of California, Irvine, California 92697

Received: February 25, 2002; In Final Form: June 24, 2002

The second-order Møller−Plesset ab initio electronic structure method is used to compute points for the anharmonic mode-coupled potential energy surface of *N*-methylacetamide (NMA) in the $trans_{ct}$ configuration, including all degrees of freedom. The anharmonic vibrational states and the spectroscopy are directly computed from this potential surface using the correlation corrected vibrational self-consistent field (CC-VSCF) method. The results are compared with CC-VSCF calculations using both the standard and improved empirical Amber-like force fields and available low-temperature experimental matrix data. Analysis of our calculated spectroscopic results show that (1) the excellent agreement between the ab initio CC-VSCF calculated frequencies and the experimental data suggest that the computed anharmonic potentials for *N*-methylacetamide are of a very high quality. (2) For most *trans*itions, the vibrational frequencies obtained from the ab initio CC-VSCF method are superior to those obtained using the empirical CC-VSCF methods, when compared with experimental data. However, the improved empirical force field yields better agreement with the experimental frequencies as compared with a standard AMBER-type force field. (3) The improved empirical force field in particular overestimates anharmonic couplings for the amide II mode, the methyl asymmetric bending modes, the out-of-plane methyl bending modes, and the methyl distortions. (4) Disagreement between the ab initio and empirical anharmonic couplings is greater than the disagreement between the frequencies, and thus the anharmonic part of the empirical potential seems to be less accurate than the harmonic contribution. (5) Both the empirical and ab initio CC-VSCF calculations predict a negligible anharmonic coupling between the amide I and other internal modes. The implication of this is that the intramolecular energy flow between the amide I and the other internal modes may be smaller than anticipated. These results may have important implications for the anharmonic force fields of peptides, for which *N*-methylacetamide is a model.

Introduction

There has been a long-standing interest in the spectroscopy and dynamics of *N*-methylacetamide (NMA). This is due in part because NMA can serve as a simple model for the amide bond in peptides and proteins. The importance of the amide group lies in its contribution to both intramolecular backbone hydrogen-bonding and solvent−protein hydrogen bonding. To accurately represent the physics of the amide bond, it is critical to first understand the intramolecular forces and the anharmonic mode coupling of this amide group. These two physical properties can have a dramatic effect on the anharmonic vibrational spectroscopy. Moreover, because experiential vibrational spectroscopy is inherently anharmonic, it is also important to understand the anharmonic effect from a theoretical perspective. In short, any such theoretical study of *N*-methylacetamide should not only include the energetics of different conformers, but also the anharmonic vibrational spectroscopy and the effects of intramolecular vibrational mode coupling. Only by comparing calculated harmonic and anharmonic vibrational frequencies with those obtain from experimental data, can we begin to gauge the importance of the anharmonic effect, and the reliability of the underlying molecular force field.

One can, in principle, measure vibrational frequencies quite accurately with low-temperature vibrational spectroscopy, either in rare gas matrixes,[1] in a nozzle jet expansion,[2−7] or in He droplets.[8−10] This is because at lower temperatures the effects of line broadening and frequency shifting will be minimized. For example, in the recent superfluid He droplet experiments of Huisken et. al,[1] the authors could spectroscopically resolve different conformers of glycine, on the OH stretching frequency. When the OH in glycine is internally hydrogen-bonded, the frequency is red shifted by 300 cm^{-1}.[1] Furthermore, recent developments in the field of two-dimensional infrared spectroscopy show substantial promise in the ability to, not only ascertain anharmonic shifts in vibrational frequencies, but also to resolve mode-coupling effects.[11−17] This newly emerging

10.1021/jp025633+ CCC: $22.00
Published on Web 08/16/2002

experimental field requires a companion in the theoretical understanding of anharmonic mode-coupled vibrational spectroscopy which we address by employing the correlation corrected vibrational self-consistent field (CC-VSCF) method in the calculation of anharmonic vibrational spectroscopy.

While the calculation of harmonic frequencies can be carried out by essentially standard routines, the calculation of anharmonic frequencies for all but the smallest polyatomic molecules presents a major challenge. To determine the anharmonic frequencies and relative degree of mode coupling in the system of interest, one can perform a vibrational self-consistent field (VSCF) calculation. This has proven to be quite accurate and useful for a wide variety of problems such as $(Ar)_{13}$ clusters,[18] peptide−water complexes,[19] glucose,[20] and BPTI hydrated with almost 200 water molecules.[21] Moreover, by extending the VSCF method using perturbation-correction treatments, Jung and Gerber were able to deal quite successfully with the highly anharmonic coupled mode system, $(H_2O)_n$, $n \leq 8$.[18] Obviously, this method is as successful as the underlying analytical force field is accurate. Until recently, only analytically available empirical force fields were used in the calculation of spectroscopy at an anharmonic level for all but very small molecules. Recently, Chaban et al.[22] have developed an algorithm that combines calculated anharmonic vibrational spectroscopy with direct calculation of ab initio potentials. This method accounts for the anharmonicities and coupling between vibrational modes using the correlation corrected vibrational self-consistent field (CC-VSCF) approach. This method does not require a fitting of an analytic potential function, nor high order derivatives. Thus, direct calculation of the anharmonic vibrational spectroscopy is feasible for molecules up to 15 atoms. The direct ab initio VSCF method was successfully applied to the calculation of the fundamental excitations of a number of hydrogen-bonded systems,[23] different conformers of glycine,[24] and a glycine−water complex.[25]

It is our aim to apply this method to the calculation of the anharmonic vibrational spectrum of *trans*-*N*-methylacetamide. Notwithstanding the depth and detailed experimental[26−35] and theoretical[36−43] investigations of *N*-methylacetamide, relatively little is still known about the intramolecular anharmonic coupling between different vibrational modes and its effect on spectroscopy. Previous high-level ab initio theoretical calculations of *N*-methylacetamide treated the spectroscopy at the harmonic level.[27,32,34,36,37,43−45] However, vibrational frequencies obtained at the harmonic level, without resorting to scaling procedures, are insufficient for a direct comparison with the experimental data. To bring the theoretical calculations of vibrational frequencies into better agreement with the experimental frequencies, a variety of scaling techniques may be employed.[46−48] Some of the extensively applied scaling methods use essentially empirical prescriptions that predict the anharmonic frequency values from the harmonically computed ones.[46] That is to say, the anharmonic contributions to the spectra includes information regarding the anharmonic part of the potential, which is of great interest. This is neglected in a harmonic calculation. However, a direct comparison of the theoretical calculations with the experimental data can be made, provided that these calculations incorporate this important anharmonic effect.

Regardless of the merits of different scaling methods in predicting anharmonic vibrational frequencies, it is important to note that these methods do not address the problem treated here, which is to compute the anharmonic spectroscopy *directly* from the ab initio anharmonic potential energy surface. We aim only to provide a computational method that does not rely on scaling. Furthermore, because the current ab initio method includes anharmonic effects, we can also gauge the degree of intramolecular mode coupling. Finally, a comparison of the ab initio anharmonic frequencies with the anharmonic frequencies obtained from calculations using an empirical force field will further illustrate the power, and limitations, of using such force fields for intramolecular vibrational energy redistribution (IVR/VET) processes. This work represents a continuing investigation into the nature of anharmonic coupling in biological molecules, and can be directly compared to experimentally determined two-dimensional vibrational spectra.

The paper is organized as follows: A general discussion of the vibrational self-consistent field method is given in section II. Section II, part A, will outline the empirical force field and the empirical VSCF method, while part B will discuss the ab initio VSCF method and the energy calculations. The results and a discussion is given in section III and the conclusions follow in section IV.

II. Vibrational Self-Consistent Field Method (VSCF) and Correlation-Corrected VSCF

Consider the vibrational Schrödinger equation:

$$\left[-\frac{\hbar^2}{2}\sum_{j=1}^{N}\frac{\partial^2}{\partial Q_j^{\,2}} + V(Q_1, ..., Q_N)\right]\Psi(Q_1, ..., Q_N) = E\Psi(Q_1, ..., Q_N) \quad (2.1)$$

treated here in mass-weighted normal mode coordinates, where Q_j is the jth mass-weighted normal mode coordinate and $V(Q_1, ..., Q_N)$ is the full potential which includes anharmonicity and coupling between all of the modes. One may simplify eq 2.1 by utilizing the separable Hartree approximation, which is the basis of the VSCF method:[49−52]

$$\Psi(Q_1, ..., Q_N) = \prod_{k=1}^{N}\psi_k^{\,n}(Q_k) \quad (2.2)$$

This then leads to N single mode VSCF equations of the following form:

$$\left[-\frac{\hbar^2}{2}\frac{\partial^2}{\partial Q_k^{\,2}} + V_k^{\,n}(Q_k) - \epsilon_k\right]\psi_k^{\,n}(Q_k) = 0 \quad (2.3)$$

where the effective potential for mode k is given by:

$$V_k^{\,n}(Q_k) = \langle\prod_{l\neq k}^{N}\psi_l^{\,n}(Q_l)|V(Q_1, ..., Q_N)|\prod_{l\neq k}^{N}\psi_l^{\,n}(Q_l)\rangle \quad (2.4)$$

Equations 2.3 and 2.4 for the single mode wave functions, energies, and effective potentials must be solved self-consistently. The VSCF expression for the total energy of vibrational state n is thus a sum of all the individual mode energies minus a term which accounts for the double counting of the interactions in the energy calculation and has the following form:

$$E_{\text{total}}^{\,n} = \sum_{k=1}^{N}\epsilon_k^{\,n} - (N-1)\langle\prod_{k=1}^{N}\psi_k^{\,n}|V(Q_1, ..., Q_N)|\prod_{k=1}^{N}\psi_k^{\,n}\rangle \quad (2.5)$$

To account for correlation effects between modes, an effective perturbation treatment analogous to Møller−Plesset method (MP2) for electronic structure calculations, is employed. In this

treatment, the expression is up to second-order perturbation in ΔV, and is as follows:

$$\Delta V(Q_1, ..., Q_N) = V(Q_1, ..., Q_N) - \sum_{k=1}^{N} V_k{}^n(Q_k) \quad (2.6)$$

The second-order correlation-corrected approximation for the energy is

$$E_n{}^{cc} = E_n{}^{VSCF} + \sum_{m \neq n} \frac{|\langle \prod_{k=1}^{N} \Psi_k{}^n(Q_k) | \Delta V | \prod_{k=1}^{N} \Psi_k{}^m(Q_k) \rangle|^2}{E_n{}^0 - E_m{}^0} \quad (2.7)$$

In eq 2.7 we assume that there are no degenerate excited states (n,m), with energy $E_n{}^0 = E_m{}^0$. The theory behind the correlation-corrected VSCF (CC-VSCF) approximation can be found in refs 49 and 51. In this case, we find, an overall improvement in the calculation of the fundamental excitations to be roughly between 5 and 10 cm^{-1} using the CC-VSCF method, compared with the VSCF method. However, the difference can be as high as 50 cm^{-1} (CO ipb CCH_3 r).

Equation 2.1 assumes the rotational state of the molecule, J, to be zero, such that the contribution of the vibrational angular momentum (i.e., Coriolis coupling) to the kinetic energy of vibration is negligible. At lower excitations of the vibrational angular momentum, the contribution to the total energy may still be small.[53] An example of this effect was recently reported for the calculation of the anharmonic vibrational spectrum for H_2O.[54] In this work, Wright and Gerber found that the maximum effect of adding Coriolis coupling to the anharmonic calculations was to increase the accuracy of the frequencies by 14 cm^{-1}.[54] In total, for the H_2O system, the maximum error in the calculated anharmonic frequencies was 34 cm^{-1}, of which 20 cm^{-1} came from the CC-VSCF approximations, and 14 cm^{-1} from neglect of vibrational angular momentum. Another example of including vibrational angular momentum (up to one quantum of excitation) in the calculation of the anharmonic vibrational energies for HCN/HNC can be found in ref 55. We believe that the relatively large mass of the present system will further decrease the effect of Coriolis coupling as compared to the H_2O system. Therefore, we have neglected the effect of vibrational angular momentum in the present calculation.

A. An Expansion Approach to the CC-VSCF Method for Analytically Available Force Fields. In the present study we utilized an empirical potential which is based on an Amber type of force field. Amber is one of the more widely used force fields in many biological studies.[55,56] The functional form for the analytical potential is as follows:[57]

$$V(\vec{R}) = \sum_{\text{bonds}} K_r(r - r_{eq})^2 + \sum_{\text{angles}} K_\theta(\theta - \theta_{eq})^2 + \sum_{\text{dihedrals}} \frac{V_n}{2}[1 + \cos(n\phi - \gamma)] + \sum_{i<j} \left[\frac{A_{ij}}{R_{ij}{}^{12}} - \frac{B_{ij}}{R_{ij}{}^6} + \frac{q_i q_j}{\epsilon R_{ij}} \right] + \sum_{i<j} \left[\upsilon_{14} \left(\frac{A_{ij}}{R_{ij}{}^{12}} - \frac{B_{ij}}{R_{ij}{}^6} \right) + \text{el}_{14} \frac{q_i q_j}{\epsilon R_{ij}} \right] \quad (2.A.1)$$

Here $\vec{R}$ is a vector containing the x,y,z coordinates of all the atoms, r represents the norm of the bonding vector between any two connected atoms, and θ is the angle between any three bonded atoms. The dihedral angle, ϕ, includes both proper and improper torsion, where γ is a phase factor and V_n is the torsional barrier parameter. The last two terms in eq 2.A.1 represent the van der Waals ($\upsilon_{14} = 8$) and electrostatic interactions ($\text{el}_{14} = 1.2$), which are calculated between atoms of either different molecules, or on the same molecule but separated by at least 3 bonds. R_{ij} is defined as the distance between atoms i and j, A_{ij}, B_{ij} are the van der Waals parameters, and q_i is the partial charge on atom i. This force field is based on the work of Cornell et al.[55,56] and is adjusted to fit the experimental vibrational spectrum of *trans*-*N*-methylacetamide.[33,37] We accomplished this fitting by varying both the torsional parameters as well as the partial charges on the methyl group atoms. A Monte Carlo search was performed on the adjustable parameters, in conjunction with a VSCF calculation of the vibrational frequencies for the fundamental excitations only, to reach better agreement with the experimental data. The best fit molecular parameters for the implementation of the improved empirical force field can be found in Table 1. Thus, the remaining differences between the calculated anharmonic frequencies and the experimental frequencies represent limitations of the basic analytical force field that cannot be overcome by a simple parameter optimization.

It should be noted that the functional form of the empirical force field is harmonic in nature for the description of the bonding and angular terms, however the nonbonding interactions are anharmonic. This could in fact be a limitation of the current force field. However, no attempt was made to change the functional form of the AMBER potential. Instead, anharmonicity was treated solely in the calculation of the vibrational frequencies. An equally valid and interesting approach would be to alter the functional form of the empirical force field to directly include additional anharmonic effects.

Assuming the system is not extremely anharmonic we can apply a power expansion about an equilibrium position to obtain the VSCF effective potential, $V_k(Q_k)$ of eq 2.4. Here $V_k(Q_k)$ is calculated by averaging, or integrating, over all the other $l \neq k$ modes as follows:

$$V_k(Q_k) = \frac{1}{2}\frac{\partial^2 V}{\partial Q_k{}^2} Q_k{}^2 + \frac{1}{6}\frac{\partial^3 V}{\partial Q_k{}^3} Q_k{}^3 + \frac{1}{24}\frac{\partial^4 V}{\partial Q_k{}^4} Q_k{}^4 + \frac{1}{2}\sum_{l \neq k}^{N} \frac{\partial^3 V}{\partial Q_k{}^2 Q_l} Q_k{}^2 \langle \psi_l(Q_l) | Q_l | \psi_l(Q_l) \rangle + \frac{1}{2}\sum_{l \neq k}^{N} \frac{\partial^3 V}{\partial Q_k Q_l{}^2} Q_k \langle \psi_l(Q_l) | Q_l{}^2 | \psi_l(Q_l) \rangle + \frac{1}{4}\sum_{l \neq k}^{N} \frac{\partial^4 V}{\partial Q_k{}^2 Q_l{}^2} Q_k{}^2 \langle \psi_l(Q_l) | Q_l{}^2 | \psi_l(Q_l) \rangle \quad (2.A.2)$$

Here, the effective potential is based on an expansion (Taylor Series) up to fourth order about a local/global minimum. In our present calculation we have neglected the cubic and higher order terms with non repeating indices ($Q_k Q_l Q_m$, $Q_k Q_l Q_m Q_n$) as they will be exceedingly small and in fact vanish in a perturbation treatment which uses the harmonic approximation as the unperturbed Hamiltonian.[58] For $n > 2$ the expansion coefficients, $\partial^n V/\partial Q_k{}^n$, were calculated using finite differences.[59] The quartic expansion (eq 2.A.2), suffices for such systems, if one studies low-lying vibrational states, and if the molecule is only moderately anharmonic. However, some systems do exhibit

TABLE 1: Molecular Mechanical Parameters

Bond Parameters

bond	K_r [kcal/(mol Å^2)]	r_{eq} (Å)
C_α−H	340.0	1.09
C−C_α	317.0	1.522
C−O	570.0	1.229
C−N	490.0	1.335
N−H	434.0	1.01
N−C_α	337.0	1.449
C_α−H	340.0	1.09

Angle Parameters

angle	K_θ [kcal/(mol radian^2)]	θ_{eq} [deg]
CO−C_α−H	40.0	109.5
CO−NH−C_α	50.0	121.9
C_α−CO−OC	80.0	120.4
C_α−NH−HN	30.0	118.04
C_α−CO−NH	70.0	116.60
H− C_α−H	38.0	109.5
OC−CO−NH	80.0	122.9
CO−NH−HN	20.0	120.0
CO−C_α−H	40.0	109.5
CO−NH−C_α	50.0	121.90
C_α−CO−OC	80.0	120.4
H−C_α−NH	40.0	109.5
H− C_α−H	38.0	109.5
H−C_α−H	38.0	109.5

Torsional Parameters

torsion	$V_n/2$ (kcal/mol)	n, periodicity of torsion	γ (deg)
H−C_α−CO−OC	0.0	2	0.0
H−C_α−CO−NH	0.0	2	0.0
CO−NH−C_α−H	0.0	2	0.0
HN−NH−C_α−H	0.0	2	0.0
OC−CO−C_α−NH	0.1	3	180
OC−CO−NH−C_α	2.5	2	180
CO−C_α−OC−NH	2.5	2	180
OC−CO−NH−HN	2.0	1	0.0
CO−NH−C_α−H	0.0	2	90
NH−C_α−CO−OC	0.0	2	0.0

Improper Torsional

torsion	K_ϕ [kcal/(mol radians^2)]	ϕ_{eq} [deg]
CO−C_α−OC−NH	100.0	0.0
NH−CO−HN−C_α	45.0	0.0

van der Waals Parameters and Charges

atom type	R^*	ϵ	charge
H	1.387	0.0157	0.100
C−C_α	1.908	0.1094	−0.36620
N−C_α	1.908	0.1904	−0.1500
CO	1.908	0.105	0.59730
OC	1.6612	0.21	−0.56790
NH	1.824	0.17	−0.41570
HN	1.487	0.0157	0.27190

strong anharmonic effects, as illustrated for $(H_2O)_n$ clusters,[60] in which case the expansion method fails completely. For this system, a grid-based method is superior to an expansion-based method. In the case of NMA, numerical test indicated that the expansion method and the grid method were equivalent, however the grid-based method requires less CPU time, and thus was chosen. The grid-based method is equivalent to the method presented in section B, for the ab initio potential.

In our present calculation, we solved each single mode VSCF Hamiltonian (eq 2.3) using the collocation method of Yang and Peet.[61] For an adjustable grid, sensitive to each mode, we choose to work in the dimensionless variable, $\bar{q}_k$, where

$$\bar{q}_k = \frac{Q_k}{(\lambda_k)^{1/4}} \tag{2.A.3}$$

Here λ_k is the kth eigenvalue of the Hessian. Convergence was determined when $[\Delta\Sigma_k[\epsilon_k]] \leq 0.0001$ kcal/mol from one iteration to the next.

B. Ab Initio Vibrational Self-Consistent Field Method. The calculation of the effective potential, eq 2.4, in an ab initio method would scale unfavorably (in CPU time) if one were to apply a Taylor Series expansion about a given configuration. Therefore, the approach taken was to assume that the potential function can be well represented by including interactions between only pairs of modes, and calculating the ab initio potential on a two-dimensional grid.[18,60] Numerical test indicated that the pair-interaction approximation used in the ab initio calculation, and the expansion method (eq 2.A.2) used for the empirical force fields, were nearly equivalent. Our experience with the pair-interaction approximation, which neglects direct coupling between triplets of normal modes, has been encouraging.[22−24] Addition of three mode coupling for small molecules such as H_2O and $Cl^-(H_2O)$ have found that the additional triplet coupling effect will alter the frequency by as much as 30 cm^{-1} in the case of the strongest OH stretch in H_2O.[23] However, the three body interaction had relatively little effect on the other frequencies in the case of H_2O.[23] While it is in principle important to include higher body interactions, it should be noted that the size of the present molecule (12 atoms) realistically would preclude the calculation of the triplet coupling between modes. In this pairwise coupling approximation, the effective potential becomes:

$$V(Q_1, ..., Q_N)\sum_{j=1}^{N} V_j(Q_j) + \sum_{i\leq j} V_{ij}(Q_i, Q_j) \tag{2.B.1}$$

where

$$V_j(Q_j) = V(Q_1 = 0, ..., Q_j, ..., Q_N = 0)$$

and

$$V_{ij}(Q_i,Q_j) = V(Q_1 = 0, ..., Q_i, Q_j, ..., Q_N = 0) \tag{2.B.2}$$

We stress that our numerical tests for several biological molecules have shown that the pairwise approximation seems valid for such molecules, and that adding additional coupling approximations of normal modes does not make a significant contribution in terms of the calculated frequencies for most systems studied.

An electronic structure calculation is first used to calculate the equilibrium configuration. Then from diagonalization of the Hessian at this configuration, the normal mode coordinates are obtained. To calculate the potential at each normal mode point, a *trans*formation back to Cartesian coordinates is made, and the potential energy is then calculated at this displaced geometry. The diagonal and mode−mode pair-coupling potentials of eq 2.B.2 were calculated on a 8-point and 8 × 8 grid which were later interpolated to a 16-point and 16 × 16 grid.

Finally, the IR intensities are calculated using the dipole moment estimated along the normal coordinate and the CC-

VSCF wave functions for the ground and excited vibrational states as[23]

$$I_i = \frac{8\pi^3 N_A}{3hc}\omega_i|\langle\Psi_i^0(Q_i)|\vec{\mu}(Q_i)|\Psi_i^1(Q_i)\rangle|^2 \quad (2.B.3)$$

In eq 2.B.3, ω_i is the CC-VSCF vibrational frequency for mode i and $\Psi_i^0(Q_i)$, $\Psi_i^1(Q_i)$ are the ground and excited-state CC-VSCF wave functions.

All ab initio calculations were performed using the GAMESS electronic structure program,[62] with second-order Møller−Plesset perturbation theory (MP2). The basis set used was a Dunning−Hay double-ζ + polarization (DZP).[63] This level of theory was found to give satisfactory results for previous ab initio-VSCF calculations on small biological molecules: glycine[24] and a glycine−water complex.[25] The number of ab initio single-point energy calculations required for both the diagonal and pair-coupling potentials is

$$N_{points} = N_{mode}N_{grid} + \frac{N_{mode}(N_{mode}-1)}{2}N_{grid}^2 \quad (2.B.4)$$

where N_{mode} is the number of normal modes, which in this case is 30, and N_{grid} is the number of grid points in one dimension. For the present calculation the number of points, on an eight-point grid, is 28 080.

III. Results and Discussion

In this work, anharmonic vibrational states and frequencies of *N*-methylacetamide were obtained for three potentials; a standard AMBER force field, an improved empirical force field calculated to agree with existing vibrational frequencies of this system, and the MP2/DZP ab initio anharmonic potential energy surface. For each of these potentials the first step involved computing the equilibrium structure. The starting structure was found from a simulated annealing simulation of the isolated *N*-methylacetamide using our modified empirical force field (Table 1). In this case the starting temperature of 300 K was slowly decreased to 5 K during the course of a 15 ps dynamics run with a time step of 15 fs. The resulting low energy structure (*trans*-NMA_{cc}) was further minimized using a steepest descents method until the norm of the forces were ≤ 0.0001. In general, There are four conformers of *trans*-NMA, corresponding to the rotation of the two methyl groups, *cis* and *trans* relative to the NH and CO groups. These conformers are very close in energy (within 1 kcal/mol).[64,65] In all previous ab initio calculations, the *trans*$_{ct}$-NMA conformer is found to be the lowest energy structure.[37,43,64,65] At this level of theory (MP2/DZP), our current calculations for all conformers of *trans*-NMA are consistent with the previous ab initio calculations. Although energetics were calculated for all conformers of *trans*-NMA, only the lowest energy structure (*trans-ct*-NMA) was used for the vibrational analysis, and is illustrated in Figure 1.

Previous ab initio calculations of Mirkin and Krimm found a 0.01 kcal/mol energy difference between *trans*-NMA_{cc} and *trans*-NMA_{tc}.[37,43] By adiabatically mapping the rotation of the CO methyl group and minimizing using the improved empirical force field, we find the barrier of rotation from *cis*−*trans* to *cis*−*cis* to be 0.23 kcal/mol. In a similar manner, the barrier of rotation from *cis*−*cis* to *trans-cis* was found to be 0.65 kcal/mol. We also find that the energy difference between the *cis*−*cis* and *trans*−*cis* structures is 0.18 kcal/mol using the adjusted empirical force field. Our calculated energy difference on the improved empirical surface between the amide bond as *cis* or *trans* in *N*-methylacetamide is 4.5 kcal/mol in favor of the *trans* conformer. Ataka and co-workers measured an enthalpic difference between the *trans* and *cis* amide bond conformers to be 1.3 kcal/mol,[33] and previous ab initio results suggest an energy difference of between 2.5 and 3.4 kcal/mol between these two structures.[37,65] Our current MP2/DZP ab initio calculations suggest an energy difference of 2.48 kcal/mol, in complete agreement with the previous ab initio calculations of Mirkin and Krimm.[36,37,43]

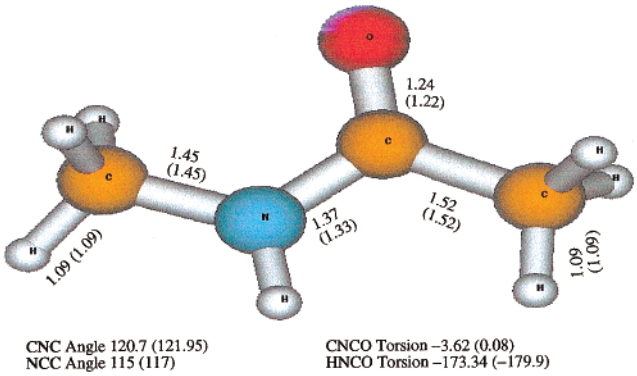

Figure 1. The optimized equilibrium structure of *trans-N*-methylacetamide. Bond lengths (in ångstroms) and angles (in degrees) are given for the ab initio MP2/DZP and empirical (in parentheses) optimized structure of NMA.

Due to the length of time required to calculate the ab initio VSCF potential energy surfaces, we only calculated the anharmonic vibrational frequencies for the *trans* − NMA_{ct} configuration (Figure 1). The original empirical CC-VSCF, adjusted empirical CC-VSCF, ab initio CC-VSCF, and the observed matrix isolated experimental frequencies are compared in Table 2, while the harmonic frequencies for all calculations are given in Table 3. The frequency assignments are also given in Tables 2 and 3. The frequency assignments were made by a comparison of the eigenvector dot product (for each normal mode compared to each normal mode) between the empirical and ab initio calculations. That is to say, for each ab initio normal mode eigenvector, we obtain a dot product with each empirical normal mode eigenvector. In general, the eigenvector dot product unambiguously assigns each normal mode between the two force fields; however, six normal modes were rather difficult to assign as the dot product between the eigenvectors was less than 0.6. These frequencies are marked with an asterisk in Tables 2 and 3 and a visual assignment was made for these cases. The experimental frequencies were obtained in a low-temperature nitrogen matrix (20K) as reported by Ataka.[33] We find, in general, that the average difference between the experimental and CC-VSCF calculated frequencies to be 133 cm^{-1} (ab initio, harmonic), 70 cm^{-1} (empirical, harmonic), 10 cm^{-1} (ab initio, CC-VSCF), and 13 cm^{-1} (empirical, CC-VSCF) from Tables 2 and 3. *It is important to mention that in the ab initio method used, scaling of the calculated (anharmonic) frequencies was not necessary since they were obtained directly from the potential*. Indeed, the advantage of the CC-VSCF method is that the anharmonic corrections are calculated from the anharmonic part of the potential, which is their true physical origin. We find the difference in the frequencies between the harmonic and CC-VSCF calculations to be as high as 300 cm^{-1} (Table 3). One can expect that, in general, an error in the ab initio CC-VSCF method will be on the order of 40−60 cm^{-1}, based on previous ab initio CC-VSCF calculations,[23−25] and a CC-VSCF density

TABLE 2: Summary of CC-VSCF Frequencies for *trans*-*N*-Methylacetamide

empirical	adjusted empirical	ab initio	observed (matrix)[33]	mode number	assignment[a]
3309	3310	3523	3498	1	NH stretch
2986	2985	2993	3008	2	CCH_3 as
2985	2986	2985	2978	3	NCH_3 as
2984	2985	3014	3008	4	CCH_3 as
2985	2986	2979	2973	5	NCH_3 as
2872	2873	2940	2958	6	NCH_3 ss
2868	2869	2939	2915	7	CCH_3 ss
1676	1662	1751	1708	8	amide I
1598	1569	1547	1511	9	amide II
1459	1462	1566	1472	10	NCH_3 ab
1459	1459	1541	1446	11	CCH_3 ab
1461	1461	1557	1446	12	NCH_3 ab
1453	1454	1515	1432	13	CCH_3 ab
1466	1465	1468	1419	14	NCH_3 sb
1388	1371	1421	1370	15	CCH_3 sb
1231	1183	1283	1265	16	amide III
1143	1148	*1214	1181	17	NCH_3 r, CN s, NH ipb
1042	1033	*1184	1089	18	CN s NCH_3r
1029	1031	1119	1037	19	CO opb CCH_3r
990	983	*1083		20	NCH_3r
956	954	1022	990	21	CCH_3r CC s
947	950	*891	857	22	CH_3 r CNC d
799	789	*637	658	23	CO ipb CC s
687	686	636	626	24	CO opb
440	402	439	439	25	CCN d CO ipb CCH_3 r
577	571	*487	391	26	CO ipb CCH_3 r
302	281	299	279	27	CNC d
227	234	245		28	CNC d NH opb
398	398	266		29	NCH_3 d
372	381	166		30	CCH_3 d

[a] s = stretch, as = asymmetric stretch, ss = symmetric stretch, d = deformation, r = rocking, ab = asymmetric bend, sb = symmetric bend, ipb = in-plane bend, opb = out-of-plane bend.

TABLE 3: Summary of Harmonic Frequencies for *trans*-*N*-Methylacetamide[a]

empirical	adjusted empirical	ab initio	observed (matrix)[33]	mode number	assignment
3316	3316	3751	3498	1	NH stretch
2992	2992	3261	3008	2	CCH_3 as
2992	2992	3248	2978	3	NCH_3 as
2991	2991	3245	3008	4	CCH_3 as
2992	2992	3225	2973	5	NCH_3 as
2878	2878	3124	2958	6	NCH_3 ss
2875	2875	3133	2915	7	CCH_3 ss
1679	1666	1780	1708	8	amide I
1597	1567	1584	1511	9	amide II
1447	1447	1548	1472	10	NCH_3 ab
1457	1457	1526	1446	11	CCH_3 ab
1453	1453	1520	1446	12	NCH_3 ab
1453	1453	1508	1432	13	CCH_3 ab
1465	1464	1484	1419	14	NCH_3 sb
1380	1359	1438	1370	15	CCH_3 sb
1218	1169	1309	1265	16	amide III
1134	1132	*1208	1181	17	NCH_3 r CN s NH ipb
1021	1010	*1173	1089	18	CN s NCH_3r
984	984	1133	1037	19	CO opb CCH_3r
968	952	*1074		20	NCH_3r
927	922	1020	990	21	CCH_3r CC s
903	903	*890	857	22	CH_3 r CNC d
793	780	*634	658	23	CO ipb CC s
661	659	624	626	24	CO opb
437	399	428	439	25	CNC d CO ipb CCH_3 r
575	569	*362	391	26	CO ipb CCH_3r
295	272	270	279	27	CNC d
217	219	153		28	CNC d NH opb
361	360	68		29	NCH_3 d
351	351	53		30	CCH_3 d

[a] s = stretch, as = asymmetric stretch, ss = symmetric stretch, d = deformation, r = rocking, ab = asymmetric bend, sb = symmetric bend, ipb = in-plane bend, opb = out-of-plane bend.

functional calculation, that included a critical analysis of errors.[54] Thus the anharmonicities of the vibrational modes of *N*-methylacetamide are quite large.

From Table 2 it is clear that the ab initio CC-VSCF method is superior to both the original and adjusted empirical CC-VSCF calculations. This is particularly true in the case of the amide I, II and III modes (1700 to 1265 cm^{-1}), which are thought to play a role in intramolecular energy redistribution pathways. The improved empirical CC-VSCF calculated frequencies for the amide I, II and III are 1662, 1569 and 1183 cm^{-1} respectively. This is compared to the calculated ab initio CC-VSCF frequencies of 1751, 1547 and 1283 cm^{-1} and the experimental frequencies of 1708, 1511 and 1265 cm^{-1}. Both empirical force fields were originally derived for solvated peptide groups. In solution, the observed *N*-methylacetamide amide I, II and III frequencies shift to 1622, 1580 and 1315 cm^{-1}.[37] The empirical force fields studied in the present work have difficulty in reproducing matrix-isolated NMA vibrational frequencies, particularly in this region. This represents a general shortcoming for most empirical force fields used to study high-resolution gas phase or matrix isolated vibrational spectroscopy, i.e., vibrational spectroscopy at a level where the anharmonic effects are significant. The fact that experimental data comes from spectroscopy in rare-gas matrixes, introduces an element of uncertainty, since the matrix shift effects can be substantial, as much as 40 cm^{-1}. However, in a recent paper on glycine[24] spectroscopic calculations for ab initio and empirical potentials were compared with matrix experiments *and* with experiments in superfluid He droplets (where the matrix effects are negligible). The superiority of the ab initio potential over the empirical potential was found to be even greater when the frequencies were compared with those of the superfluid He droplet experiment.

It is also clear from a comparison between Tables 2 and 3 that some vibrational modes of NMA are quite anharmonic, as seen by a comparison between the ab initio harmonic and ab initio CC-VSCF frequencies. This is particularly true for the stretching frequencies of the NH and methyl groups (3495 to 2900 cm^{-1}). The ab initio CC-VSCF method has difficulty in reproducing some of the asymmetric and symmetric bending modes of the methyl groups (1529 to 1394 cm^{-1}), most likely due to insufficient quality of the basis set used. However the ab initio CC-VSCF calculation does quite accurately capture the lower frequency modes corresponding to the in-plane and out-of-plane bends and the methyl distortions ($<$900 cm^{-1}). In this region, the empirical expansion method (eq 2.A.2) becomes less reliable. In general, the adjusted empirical anharmonic frequencies compare well with both the experimental and anharmonic ab initio frequencies for the most of the spectrum. This represents an impressive success of the empirical force field, as it was not originally designed for such calculations. However, the empirical force field is unable to accurately describe the amide I, amide II and amide III frequencies, which are an important signature for tertiary structural analysis (Table 2). This is an implicit advantage of the ab initio CC-VSCF method, the ability to quite accurately describe the anharmonicities of the amide frequencies of a peptide, without resorting to scaling.

To investigate further the degree of anharmonicity in the amide modes, we have defined a scalar quantity, the *coupling strength* (CS), which will indicate the degree of mode-to-mode-

coupling. Here the coupling strength (CS) for the $1 \leftarrow 0$ *trans*ition, is defined as

$$CS_{ij}^{1\leftarrow 0} = (0.5) \times \frac{\langle \Psi_i^0(Q_i)\Psi_j^1(Q_j)|V_{ij}|\Psi_i^0(Q_i)\Psi_j^0(Q_j)\rangle + \langle \Psi_i^1(Q_i)\Psi_j^0(Q_j)|V_{ij}|\Psi_i^0(Q_i)\Psi_j^0(Q_j)\rangle}{\hbar(\nu_j^0 - \nu_i^0)} \quad (3.1)$$

In eq 3.1, the measure of the coupling strength is dimensionless. Here we divide by the frequency difference between the modes, since in cases of near-degeneracy, the effects of a given magnitude of coupling element are much greater. Ψ_i^0 and Ψ_i^1 represent the ground and first excited-state wave functions for mode *i*. The wave functions are determined self-consistently using eq 2.3. In eq 3.1, V_{ij} is the coupling potential, defined by eq 2.B.2 (ab initio) and the off-diagonal terms of eq 2.A.2 (empirical). Tables 4 and 5, Supporting Information, give the matrix elements for the coupling strength $CS_{ij}^{1\leftarrow 0}$ for both the adjusted empirical (Table 4) and ab initio (Table 5) coupling potentials. One would read a symmetric matrix element ($CS_{ij}^{1\leftarrow 0}$) as representing the coupling strength between modes *i* and *j*.

The largest coupling strength ($CS^{1\leftarrow 0} = 4.1$) calculated using the ab initio coupling potential is between the NCH_3 asymmetric stretch and CH_3 asymmetric stretch (matrix element 2,5, Table 5). In the case of the adjusted empirical coupling potential, the degree of coupling between the NCH_3 asymmetric stretch and CH_3 asymmetric stretch is greatly reduced, even though the frequencies are nearly degenerate. This is illustrated in Figure 2, which is a comparison between the mode-to-mode coupling potentials for both the ab initio and the improved empirical force fields, as seen on a three-dimensional surface plot. The energies are given in Hartrees (*z*-axis) and the normal mode coordinates (Q_i) are in a dimensionless variable as given by eq 2.A.3. It can be seen from Figure 2 that the ab initio coupling potential is significantly larger than the empirical coupling potential, and the ab initio frequencies of these two modes are almost degenerate (14 cm^{-1} difference). Thus the probability of energy transfer between the NCH_3 asymmetric stretch and CH_3 asymmetric stretch is expected to be quite large in the ab initio case, compared to that of the adjusted empirical potential energy surface.

We also find that the amide I mode, at 1708 cm^{-1}, does not couple to other internal modes, as seen by the eighth row in both coupling strength matrixes (Tables 4 and 5). This is true for both the empirical and the ab initio coupling potentials. We believe that this may be significant for interpretation of recent experimental data. In the previous femtosecond nonlinear-infrared spectroscopic studies of Hamm and co-workers, the amide I mode of NMAD (deuterated NMA) was found to have a vibrational relaxation of 450 fs.[13] This is quite fast, and therefore it was postulated that the vibrational energy transfer was internal via an intramolecular energy redistribution (IVR) process. Transfer to the solvent should take more time and is expected to be on the order of 10−100 ps. Because Hamm and co-workers also saw similar relaxation rates for three small globular proteins, they concluded that this relaxation process is essentially the same for the amide I mode of all systems, and is an intrinsic property of the peptide group itself. They proposed that the possible candidate modes for energy transfer in NMAD could be the amide IV band at 628 cm^{-1}, the amide III mode at 965 cm^{-1} or the CO out-of-plane bend at 1044 cm^{-1}. We had originally thought that the relaxation may be a $2 \leftarrow 0$ transfer to the amide III or possibly the amide IV band, as there is no appreciable intramolecular coupling to an amide I $1 \leftarrow 0$ transition. The most likely reason for this is that the amide I frequency is not near-degenerate to any other intramolecular frequencies, and furthermore, the mode-to-mode coupling of amide I is not as strong as other calculated intramolecular couplings. Because the coupling strength is weighted by the frequency difference, this makes the probability of intramolecular vibrational energy transfer (from $1 \leftarrow 0$) unlikely for the amide I mode in NMA. However, we also calculated the $2 \leftarrow 0$ coupling element between that amide I and other intramolecular modes, and did not find any appreciable coupling to either the amide III or the amide IV. Thus, it is possible that the amide I relaxation is due to energy transfer to the solvent, or to energy transfer between modes which are not simply expressed in a pairwise fashion. We are currently investigating this further. It therefore still remains unclear which modes receive vibrational energy in such a short amount of time (450 fs).

In the case of the amide II mode, however, there is the probability of vibrational energy transfer to the other internal modes. For the ab initio case there are two likely intramolecular modes to receive energy, the NCH_3 asymmetric bend and the CCH_3 asymmetric bend (modes 10 and 11). The empirical force field also predicts that the amide II couples to the NCH_3 asymmetric bend and the CCH_3 asymmetric bend, although with different probabilities. However, in the case of the empirical force field, we also find significant coupling between the amide II and NCH_3 symmetric bend (mode 14), CO out-of-plane bend, CCH_3 rocking (mode 19), and the CCH_3 rocking, CC stretch (mode 21). To illustrate this, we make a three-dimensional plot of the coupling potentials between modes 9 and 11 (Figure 3) and modes 9 and 14 (Figure 4). The energies are given in Hartrees (*z*-axis). To illustrate the region of interest, we plot the one-dimensional ab initio computed anharmonic potential, and wave function, for the amide II mode (Figure 5). In Figure 3, it is clear that both force fields couple amide II with the *CCH*$_3$ asymmetric bend, in the region of interest. Although the calculated empirical mode-coupled potential energy curves are quite a bit larger than the corresponding ab initio calculated mode-coupled potential energy curves, the coupling strength is larger in the ab initio case. This is most likely due to the near-degeneracy (energy separation of 6 cm^{-1}) of the modes compared with an energy separation of 104 cm^{-1} between these same two modes in the empirical calculation.

In Figure 4 it is quite clear that the improved empirical coupling potential greatly overestimates the coupling between the amide II and the NCH_3 symmetric bend−NC stretch (modes 9 and 14), in the region of interest. Similar overestimations of the intramolecular coupling exist between the other two modes (9 and 19; 9 and 21) as well. In part, the strong coupling potentials to these three internal modes may explain why the empirical amide II frequency is blue shifted by 22 cm^{-1} from the ab initio frequency. If one were to simulate an intramolecular vibrational energy relaxation process (IVR) between the amide II and other internal vibrational modes using an empirical force field, the probability of an erroneous energy transfer would exist in this case. In comparison between the empirically calculated and the ab initio calculated coupling strength, we find that many mode-to-mode couplings are overestimated using the empirical force field. It is therefore quite important to compare the ab initio and empirical coupling strengths and coupling potentials, to accurately gauge possible IVR pathways.

Conclusions

In this paper, anharmonic vibrational spectroscopic calculations (CC-VSCF) were carried out for *N*-methylacetamide. The

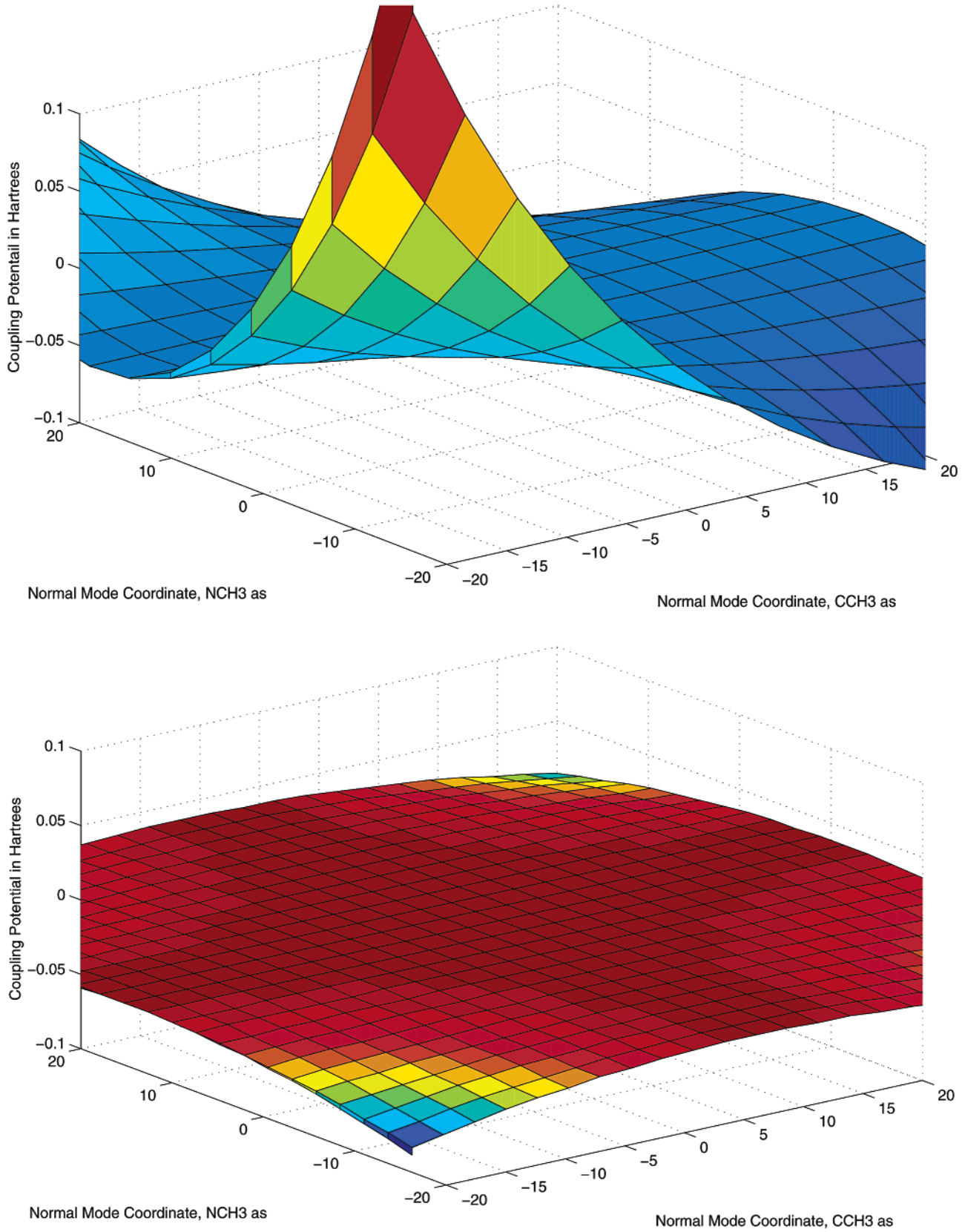

Figure 2. The coupling potential between the CCH_3 asymmetric stretch and the NCH_3 asymmetric stretch (modes 2 and 5) for the ab initio (top part) and the empirical (bottom part) force fields. The normal mode coordinates are in a dimensionless variable as given by eq 2.A.3. The coupling potential is given in Hartrees. For comparison, both potentials are given on the same scale and the color is a guide to the coupling energy.

calculations were done using three different force fields: The standard AMBER force field, an AMBER force field re-parametrized essentially to give the best possible spectroscopic agreement, and an ab initio force field, computed as a grid of many points on the multidimensional potential energy surface. Comparison of the calculated frequencies with matrix isolated

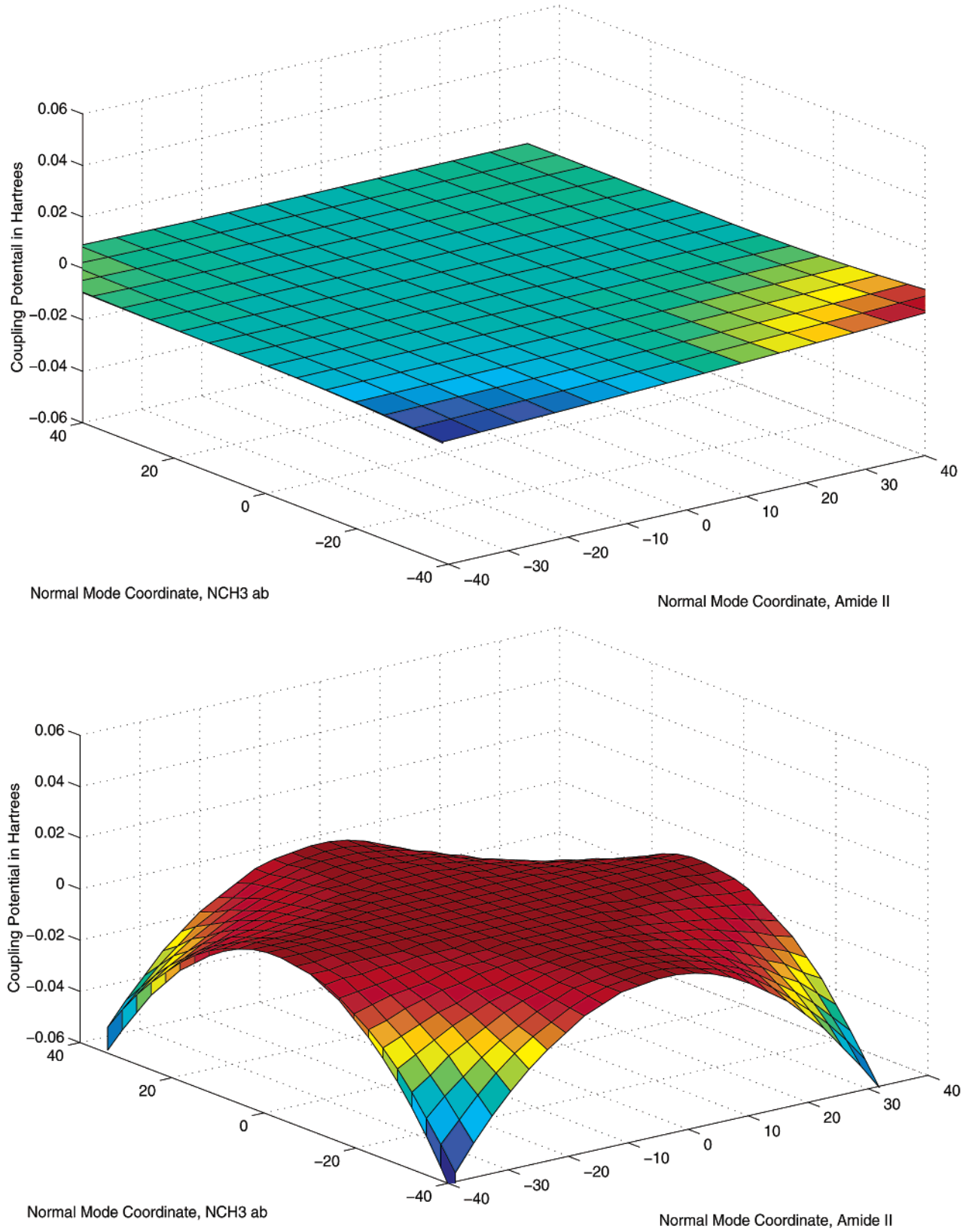

Figure 3. The coupling potential between the amide II and the CCH_3 ab (modes 9 and 11) for the ab initio (top part) and the empirical (bottom part) force fields. The normal mode coordinates are in a dimensionless variable as given by eq 2.A.3. The coupling potential is given in hartrees. For comparison, the potentials are given on the same scale and the color is a guide to the coupling energy.

experimental data makes possible an evaluation of the quality of the different force fields used. The use of the CC-VSCF method for the vibrational calculations is thus essential, since the anharmonic effects in the experimental data are important, and since it is the anharmonic part of the potential that is of the greatest interest to us.

One of the main findings of this study is that the ab initio potential surface does very well by the spectroscopic test.

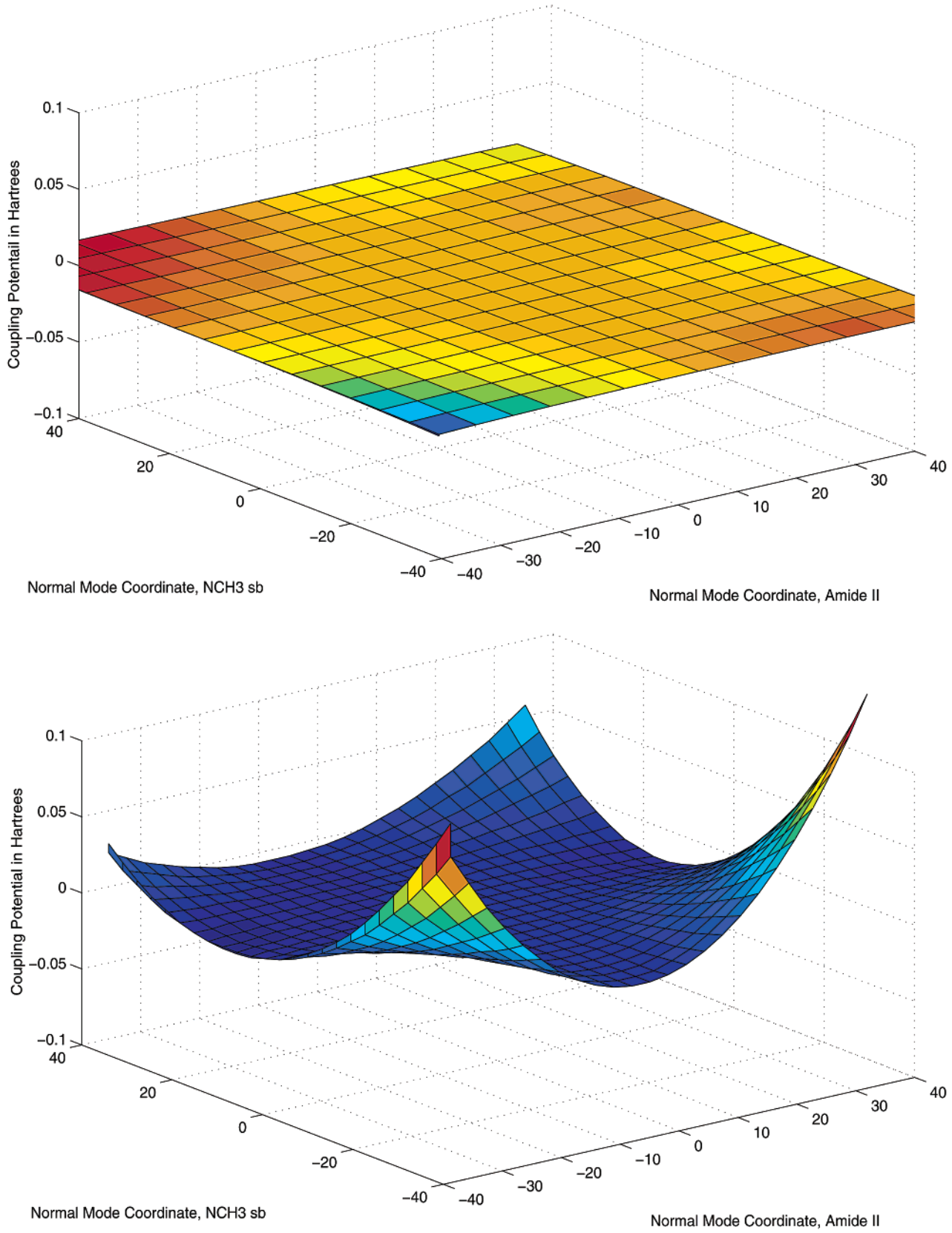

Figure 4. The coupling coupling potential between the amide II and the NCH_3 sb NC s (modes 9 and 14) for the ab initio (top panel) and the empirical (bottom panel) force fields. The normal mode coordinates are in a dimensionless variable as given by eq 2.A.3. The coupling potential is given in hartrees. For comparisons, both potentials are given on the same scale and the color is a guide to the coupling energy.

Furthermore, this potential surface yields, on the whole, better agreement with the experimental frequencies than both the standard and the spectroscopically fitted AMBER force fields. The average error for the ab initio potential, using the CC-VSCF method was 10 cm^{-1} compared to an average error of 13 cm^{-1} for the empirical potential. This result is not surprising, and is in line with the conclusions of a recent study on glycine.[24] Indeed, this is gratifying, since the present ab initio method

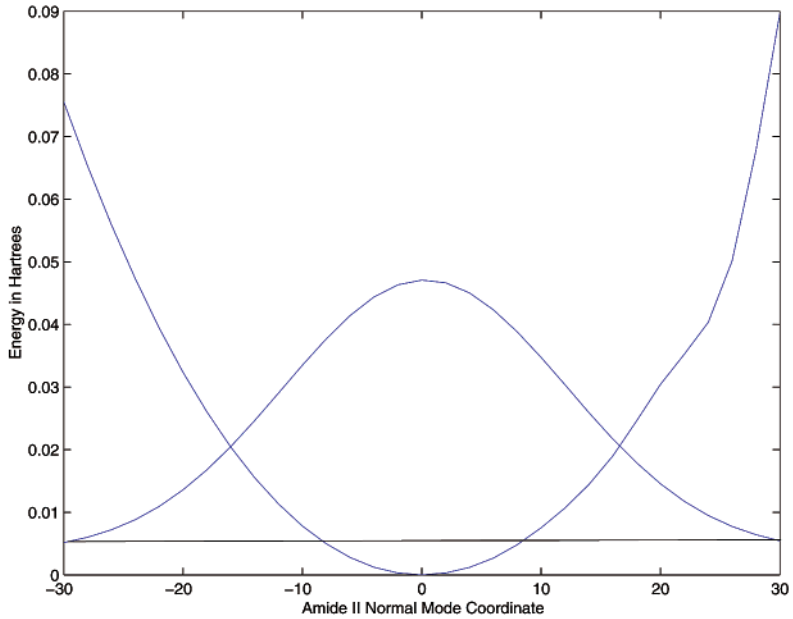

Figure 5. The ab initio anharmonic one-dimensional potential, and wave function, for the Amide II mode, as computed from the electronic structure program, GAMESS, with second-order Møller−Plesset perturbation theory (MP2). The potential is given in hartrees and the normal mode coordinate is given in a dimensionless variable as calculated using eq 2.A.3

(MP2 algorithm with a relatively modest basis set) is computationally inexpensive. The triumph of the ab initio over the empirical force fields is not uniform for all modes. This can be seen in particular for the NH stretch and the methyl bending modes. However, the amide I, amide II, and amide III modes are examples where the ab initio potential does significantly better than the AMBER force fields. We would like to point out that the spectroscopically adjusted AMBER force field is still a modest improvement over the standard AMBER force field. The improvements obtained here were just that of re-parametrizing AMBER force field parameters. Any major improvement for an empirical force field should ultimately include adjusting the functional form of the potential itself, ie to directly include additional anharmonic terms. This is a more demanding task that was not attempted here, but would be a possible future direction for producing a new generation of empirical potentials.

Another interesting finding of this work on the *N*-methylacetamide vibrations, is that the amide I fundamental excitation seems weakly coupled to other internal modes. This would seem to suggest that the fast decay observed for that excitation may be do to either solvent interactions or to other excitations not considered here.

We also find that the *anharmonic* parts of the empirical potential deviate significantly from their ab initio counterparts. This can be seen by comparing Figures 2-4. The anharmonic deviation is more pronounced than the deviation from the harmonic part of the potentials, and is a significant finding. Thus, the main improvements that are necessary in the AMBER force field are those that will improve the anharmonic interactions. Recent developments in Infrared and Raman spectroscopy can provide a basis of data for pursuing these improvements.

In this study we also defined quantities to characterize the strength of the anharmonic coupling between different normal modes. The strength of the anharmonic coupling should, as was pointed out, be greatly relevant to the flow of energy between different modes. Energy flow between different modes is not possible in a strictly harmonic approximation. On the basis of this study, we cannot expect AMBER type of potentials to describe well, and realistically, such energy flow. In attempting to describe this phenomena, in which there is a growing interest, ab initio potentials should be used, if at all possible. Alternatively, one could improve the empirical anharmonic potential energy functions. Hopefully, these conclusions may provide future directions for developing improved anharmonic force fields for small biological molecules.

Acknowledgment. We are very grateful to Drs. R. Schweitzer-Stenner, B. Brauer, and N. Wright for helpful discussions and careful reading of the manuscript. S.K.G. acknowledges a postdoctoral fellowship from the Sloan Foundation and the Department of Energy. G.M.C. acknowledges a Golda Meir postdoctoral fellowship at the Hebrew University. This work is supported in part by the US-Israel Bi-National Science Foundation (to R.G.B.). The research at UC Irvine was supported by a grant from the Molecular and Cellular Biophysics Division of NSF (Contract MCB-9982629, to R.B.G.).

Supporting Information Available: The matrix elements for the coupling strength $CS_{ij}^{1\leftarrow 0}$ for both the adjusted empirical (Table 4) and ab initio (Table 5) coupling potentials. This material is available free of charge via the Internet at http://pubs.acs.org.

References and Notes

(1) Huisken, F.; Werhahn, O.; Ivanov, A. Y.; Krasnokutski, S. A. *J. Chem. Phys.* **1999**, *111*, 2978.

(2) Davis, S.; Uy, D.; Nesbitt, D. *J. Chem. Phys.* **2000**, *112*, 1823.

(3) Uy, D.; Davis, S.; Nesbitt, D. *J. Chem. Phys.* **1998**, *109*, 7793.

(4) Votava, O.; Fair, J. D.; Plusquellic, D. F.; Riedle, E.; Nesbitt, D. J. *J. Chem. Phys.* **1997**, *107*, 8854.

(5) Anderson, D. T.; Davis, S.; Nesbitt, D. J. *J. Chem. Phys.* **1997**, *107*, 1115.

(6) Dickinson, J. A.; Hockridge, M. R.; Kroemer, R. T.; Robertson, E. G.; Simons, J. P. *J. Am. Chem. Soc.* **1998**, *180*, 2622.

(7) Hockridge, M. R.; Robertson, E. G.; Simons, J. P. *Chem. Phys. Lett.* **1999**, *302*, 538.

(8) Naura, K.; Miller, R. E. *Science* **2000**, *287*, 293.

(9) Naura, K.; Moore, D. T.; Miller, R. E. *Faraday Discuss. Chem. Soc.* **2000**, *113*, 261.

(10) Lindinger, A.; Toennies, J. P.; Vilesov, A. F. *J. Chem. Phys.* **1998**, *110*, 1429.

(11) Asplund, M. C.; Zanni, M. T.; Hochstrasser, R. M. *Proc. Nat. Acad. Sci.* **2000**, *97*, 8219.
(12) Zanni, M. T.; Asplund, M. C.; Hochstrasser, R. M. *J. Chem. Phys.* **2001**, *114*, 4579.
(13) Hamm, P.; Lim, M.; Hochstrasser, R. M. *J. Phys. Chem. B* **1998**, *102*, 6123.
(14) Hamm, P.; Lim, M.; Asplund, M.; Hochstrasser, R. M. *Proc. Nat. Acad. Sci.* **1999**, *96*, 2036.
(15) Hamm, P.; Lim, M.; Asplund, M.; Hochstrasser, R. M. *Chem. Phys. Lett.* **1999**, *301*, 167.
(16) Zhang, W. M.; Chernyak, V.; Mukamel, S. *J. Chem. Phys.* **1999**, *110*, 5011.
(17) Woutersen, S.; Hamm, P. *J. Phys. Chem. B* **2000**, *104*, 11316.
(18) Jung, J. O.; Gerber, R. B. *J. Chem. Phys.* **1996**, *105*, 10682.
(19) Gregurick, S. K.; Fredj, E.; Elber, R.; Gerber, R. B. *J. Phys. Chem.* **1997**, *101*, 8595.
(20) Gregurick, S. K.; J. Liu, H.-Y.; Brant, D. A.; Gerber, R. B. *J. Phys. Chem.* **1999**, *103*, 3476.
(21) Roitberg, A.; Gerber, R. B.; Elber, R.; Ratner, M. A. *Science* **1995**, *268*, 1319.
(22) Chaban, G. M.; Jung, J. O.; Gerber, R. B. *J. Chem. Phys.* **1999**, *111*, 1823.
(23) Chaban, G. M.; Jung, J. O.; Gerber, R. B. *J. Phys. Chem. A* **2000**, *104*, 2772.
(24) Chaban, G. M.; Jung, J. O.; Gerber, R. B. *J. Phys. Chem. A* **2000**, *104*, 10035.
(25) Chaban, G. M.; Gerber, R. B. *J. Chem. Phys.* **2001**, *115*.
(26) Schweitzer-Stenner, R.; Sieler, G.; Christansen, H. *Asian J. Phys*. **1998**, *7*, 287.
(27) Chen, X. G.; Asher, S. A.; Schweitzer-Stenner, R.; Mirkin, N. G.; Krimm, S. *J. Am. Chem. Soc.* **1995**, *117*, 2884.
(28) Sieler, G.; Schweitzer-Stenner, R.; Holtz, J. S. W.; Pajcini, V.; Asher, S. A. *J. Phys. Chem. B* **1999**, *103*, 372.
(29) Liu, Y.; Czarnecki, A. M. A.; Ozaki, Y. *Appl. Surf. Sci*. **1994**, *48*, 1095.
(30) Triggs, N. E.; Valentini, J. J. *J. Phys. Chem.* **1992**, *96*, 6922.
(31) Sieler, G.; Schweitzer-Stenner, R. *J. Am. Chem. Soc.* **1997**, *119*, 1720.
(32) Schweitzer-Stenner, R.; Sieler, G.; Mirkin, N.; Krimm, S. *J. Phys. Chem. A* **1998**, *102*, 118.
(33) Ataka, S.; Takeuchi, H.; Tasumi, M. *J. Mol. Struct.* **1984**, *113*, 147.
(34) Chen, X. G.; Schweitzer-Stenner, R.; Krimm, S.; Mirkin, N. G.; Asher, S. A. *J. Am. Chem. Soc.* **1994**, *116*, 11141.
(35) Ludwig, R.; Reis, O.; Winter, R.; Weinhold, F.; Farrar, T. C. *J. Phys. Chem. B* **1998**, *102*, 9312.
(36) Mirkin, N. G.; Krimm, S. *J. Am. Chem. Soc.* **1990**, *112*, 9016.
(37) Mirkin, N. G.; Krimm, S. *Theochem. J. Mol. Struct*. **1991**, *236*, 97.
(38) Markham, L. M.; Hudson, B. S. *J. Phys. Chem.* **1996**, *100*, 2731.
(39) Maple, J. R.; Hwang, M.-J.; Jalkanen, K. J.; Stockfisch, T. P.; Hagler, A. T. *J. Comput. Chem.* **1998**, *19*, 430.
(40) Rick, S. W.; Berne, B. J. *J. Am. Chem. Soc.* **1996**, *118*, 672.
(41) Besley, N. A.; Hirst, J. D. *J. Phys. Chem. A* **1998**, *102*, 10791.
(42) Torii, H.; Tatsumi, T.; Tasumi, M. *J. Raman Spectrosc.* **1998**, *29*,.
(43) Mirkin, N. G.; Krimm, S. *J. Am. Chem. Soc.* **1991**, *113*, 9742.
(44) Mirkin, N. G.; Krimm, S. *Theochem. J. Mol. Struct*. **1995**, *334*, 1.
(45) Herrebout, W. A.; Clou, K.; Desseyn, H. O. *J. Phys. Chem. A* **2001**, *105*, 4865.
(46) Scott, A. P.; Radom, L. J. *J. Phys. Chem. A* **1996**, *100*, 16502.
(47) Pulay, P.; Fogarasi, G.; Pongor, G.; Boggs, J. E.; Vargha, A. *J. Am. Chem. Soc.* **1983**, *105*, 7037.
(48) Allen, W. D.; Csaszar, A. G.; Horner, D. A. *J. Am. Chem. Soc.* **1992**, *114*, 6834.
(49) Gerber, R. B.; Ratner, M. A. *Adv. Chem. Phys.* **1988**, *70*, 97.
(50) Bowman, J. M. *J. Chem. Phys.* **1978**, *68*, 608.
(51) Gerber, R. B.; Ratner, M. A. *Chem. Phys. Lett*. **1979**, *68*, 195.
(52) Bowman, J. M. *Acc. Chem. Res.* **1986**, *19*, 202.
(53) Pavlyuchko, A. I.; Gribov, L. A. *Opt. Spectrosc*. **1985**, *58*, 767.
(54) Wright, N. J.; Gerber, R. B. *J. Chem. Phys.* **2000**, *112*, 2598.
(55) Weiner, S. J.; Kollman, P. A.; Case, D. A.; Singh, U. C.; Ghio, C.; Alagona, G.; Profeta, S., Jr.; Weiner, P. *J. Am. Chem. Soc.* **1984**, *106*, 765.
(56) Weiner, S. J.; Kollman, P. A.; Nguyen, D. T.; Case, D. A. *J. Comput. Chem.* **1986**, *7*, 230.
(57) Cornell, W. D.; Cieplak, P.; Bayly, C. I.; Gould, I. R.; Merz, K. M., Jr.; Ferguson, D. M.; Spellmeyer, D. C.; Fox, T.; Caldwell, J. W.; Kollman, P. A. *J. Am. Chem. Soc.* **1995**, *117*, 5179.
(58) Nielsen, H. H. *Rev. Mod. Phys.* **1951**, *23*, 90.
(59) Schneider, W.; Thiel, W. *Chem. Phys. Lett.* **1989**, *157*, 367.
(60) Jung, J. O.; Gerber, R. B. *J. Chem. Phys.* **1996**, *105*, 10332.
(61) Yang, W.; Peet, A. C. *Chem. Phys. Lett.* **1988**, *153*, 98.
(62) Schmidt, M. W.; Baldridge, K. K.; Boatz, J. A.; Elbert, S. T.; Gordon, M. S.; Jensen, J. H.; Matsunaga, N.; Nguyen, K. A.; Sa, S.; Windus, T. L.; Dupuis, M.; Montgomery, J. A. *J. Comput. Chem.* **1993**, *14*, 1347.
(63) Dunning, T. H.; Hay, P. J. *Methods of Electronic Structure Theory*; Plenum: New York, 1977.
(64) Kang, Y. K. *Theochem. J. Mol. Struct.* **2001**, *546*, 183.
(65) Nandini, G.; Sathyanarayana, D. N. *Theochem. J. Mol. Struct.* **2002**, *579*, 1.